

Simulating Diffusion Bridges with Score Matching

Valentin De Bortoli* Arnaud Doucet* Jeremy Heng^{†‡} James Thornton*

Abstract

We consider the problem of simulating diffusion bridges, i.e. diffusion processes that are conditioned to initialize and terminate at two given states. Diffusion bridge simulation has applications in diverse scientific fields and plays a crucial role for statistical inference of discretely-observed diffusions. This is known to be a challenging problem that has received much attention in the last two decades. In this work, we first show that the time-reversed diffusion bridge process can be simulated if one can time-reverse the unconditioned diffusion process. We introduce a variational formulation to learn this time-reversal that relies on a score matching method to circumvent intractability. We then consider another iteration of our proposed methodology to approximate the Doob’s h -transform defining the diffusion bridge process. As our approach is generally applicable under mild assumptions on the underlying diffusion process, it can easily be used to improve the proposal bridge process within existing methods and frameworks. We discuss algorithmic considerations and extensions, and present some numerical results.

Keywords: Diffusions, diffusion bridges, score matching, stochastic differential equations, time-reversal.

1 Introduction

Diffusion processes are a class of continuous-time models that have been extensively used in many disciplines. A diffusion process $X = (X_t)_{t \in [0, T]}$ in \mathbb{R}^d is defined by the stochastic differential equation (SDE)

$$dX_t = f(t, X_t)dt + \sigma(t, X_t)dW_t, \quad (1)$$

where $f : [0, T] \times \mathbb{R}^d \rightarrow \mathbb{R}^d$ is a drift function, $\sigma : [0, T] \times \mathbb{R}^d \rightarrow \mathbb{R}^{d \times d}$ is a diffusion coefficient and $W = (W_t)_{t \in [0, T]}$ is a d -dimensional standard Brownian motion. We suppose f and σ are sufficiently regular to induce a unique (weak) solution of (1), and $\Sigma(t, x_t) = (\sigma\sigma)^\top(t, x_t)$ is uniformly positive definite for all $(t, x_t) \in [0, T] \times \mathbb{R}^d$. For any $0 \leq s < t \leq T$, we will write the transition density of (1) with respect to the Lebesgue measure on \mathbb{R}^d as $p(t, x_t | s, x_s)$ and assume that it is positive for ease of exposition.

*Department of Statistics, University of Oxford, UK.

[†]ESSEC Business School, Singapore.

[‡]Corresponding author: heng@essec.edu

We consider the problem of simulating X when the process at the initial and terminal times is conditioned to satisfy $X_0 = x_0 \in \mathbb{R}^d$ and $X_T = x_T \in \mathbb{R}^d$, respectively. Simulating the conditioned process $X^* = (X_t^*)_{t \in [0, T]}$, commonly referred to as a diffusion bridge, is known to be a challenging problem that has received much attention in the last two decades. When performing statistical inference for parameters of f and σ in the case where X is only observed at discrete time points, diffusion bridge simulation is a crucial tool that allows one to impute missing paths between observations within an Expectation-Maximization algorithm or a Gibbs sampler (Pedersen, 1995; Roberts and Stramer, 2001; Elerian et al., 2001; Eraker, 2001; Durham and Gallant, 2002; Beskos et al., 2006; Golightly and Wilkinson, 2008; van der Meulen and Schauer, 2017). The use of diffusion bridges can also be found in diverse fields such as computational chemistry (Bolhuis et al., 2002; Wang et al., 2020), quantitative finance (Pellegrino and Sabino, 2015) and shape analysis (Arnaudon et al., 2020).

It is well-known that, under mild assumptions, the diffusion bridge X^* satisfies an SDE that is given by Doob's h -transform (Rogers and Williams, 2000, p. 83)

$$dX_t^* = \{f(t, X_t^*) + \Sigma(t, X_t^*) \nabla \log h(t, X_t^*)\} dt + \sigma(t, X_t^*) dW_t, \quad (2)$$

with initial condition $X_0^* = x_0$, where $\nabla = (\partial_{x_1}, \dots, \partial_{x_d})^\top$ denotes the gradient operator and $h(t, x_t) = p(T, x_T | t, x_t)$ is defined by the transition density of X . The term $\Sigma(t, x_t) \nabla \log h(t, x_t)$ forces the conditioned process towards the terminal condition $X_T^* = x_T$. As the transition density and hence its logarithmic gradient is intractable for most diffusions, exploiting this result to simulate diffusion bridges is highly non-trivial.

A common theme in many existing papers is to construct a proposal bridge process $X^\circ = (X_t^\circ)_{t \in [0, T]}$, satisfying

$$dX_t^\circ = f^\circ(t, X_t^\circ) dt + \sigma(t, X_t^\circ) dW_t, \quad (3)$$

using a tractable approximation of (2) that is then corrected using an importance sampler (see Papaspiliopoulos and Roberts (2012) for an overview) or independent Metropolis–Hastings algorithm (see e.g. Elerian et al. (2001)). The choice of drift function $f^\circ : [0, T] \times \mathbb{R}^d \rightarrow \mathbb{R}^d$ should be such that the law of X^* is absolutely continuous with respect to that of X° , with a Radon–Nikodym derivative that can be evaluated up to a normalizing constant. These requirements clearly preclude the simple option $f^\circ(t, x_t) = f(t, x_t)$ (Pedersen, 1995). The drift of a Brownian bridge $f^\circ(t, x_t) = (x_T - x_t)/(T - t)$ has been considered in several works (Durham and Gallant, 2002; Delyon and Hu, 2006; Stramer and Yan, 2007; Papaspiliopoulos et al., 2013), and improved by Whitaker et al. (2017) using an innovative decomposition of the process into deterministic and stochastic parts. Clark (1990) followed by Delyon and Hu (2006) studied the choice $f^\circ(t, x_t) = f(t, x_t) + (x_T - x_t)/(T - t)$ that incorporates the dynamics of the original process X . To introduce more flexibility and better mimic the structure of (3), Schauer et al. (2017) proposed setting $f^\circ(t, x_t) = f(t, x_t) + \Sigma(t, x_t) \nabla \log \tilde{h}(t, x_t)$, where $\tilde{h}(t, x_t) = \tilde{p}(T, x_T | t, x_t)$ is given by an analytically tractable transition density of an auxiliary process. For tractability, the latter is typically chosen from the class of linear processes and can be optimized to get the best approximation within this class (van der Meulen and Schauer, 2017). Other Markov chain Monte Carlo (MCMC) approaches include Gibbs sampling (Eraker, 2001), Langevin-type stochastic partial differential equations (Stuart et al., 2004; Beskos et al., 2008) and piecewise deterministic MCMC (Bierkens et al., 2021).

The exact SDE simulation algorithms developed in Beskos and Roberts (2005) and Beskos et al. (2006) can be employed to sample diffusion bridges without any time-discretization error. However, these elegant methods are limited to the class of diffusion processes that can be transformed to have unit diffusion coefficient. Bladt and Sørensen (2014) and Bladt et al. (2016) devised an ingenious methodology to simulate diffusion bridges based on coupling and time-reversal of diffusions. Their proposed method is applicable to the class of ergodic diffusions with an invariant density that is either explicitly known or numerically approximated. Closely related approaches include sequential Monte Carlo algorithms that resample using backward information filter approximations (Guarniero, 2017), information from backward pilot paths (Lin et al., 2010), or guided weight functions (Del Moral and Murray, 2015), and the methodology discussed in Wang et al. (2020). The underlying idea of these works is a characterization of the function h as the solution of the backward Kolmogorov equation

$$\partial_t h(t, x_t) + (\mathcal{L}h)(t, x_t) = 0, \quad 0 \leq t < T, \quad (4)$$

with terminal condition at time T given by the Dirac measure at x_T , where \mathcal{L} denotes the generator of X . The partial differential equation (PDE) in (4) reveals that h propagates information about the terminal constraint backwards in time. Numerical resolution of this PDE is challenging due to the singularity at time T and when the dimension d is large (Wang et al., 2020).

Our work aims to contribute to this rich body of literature by showing that it is possible to approximate some key quantities involving diffusion bridges. This was motivated by our recent work in De Bortoli et al. (2021) on a related but distinct problem of simulating Schrödinger bridges. In Section 3.1, we begin by examining the dynamics of the time-reversed bridge process X^* . This amounts to a time-reversal of the SDE in (1) which depends on the score function $\nabla_{x_t} \log p(t, x_t | 0, x_0)$. Section 3.2 introduces a variational formulation to learn this score function using a score matching method (Vincent, 2011). In Section 3.3, we explain how another iteration of this methodology can be used to obtain an approximation of the Doob’s h -transformed process in (2). As our approach is generally applicable under mild assumptions on the SDE in (1), it can easily be used to improve the proposal bridge process within existing methods and frameworks. We give algorithmic implementation details in Section 3.4 and discuss extensions of our methodology in Section 3.5. Lastly, in Section 5, we present some numerical results on an Ornstein–Uhlenbeck process and a diffusion process with periodic drift. A PyTorch implementation is available at <https://github.com/jeremyhengjm/DiffusionBridge>.

2 Notation

We write $\langle x, y \rangle_A = x^\top A y$ for the inner product of $x, y \in \mathbb{R}^d$ weighted by a positive definite matrix $A \in \mathbb{R}^{d \times d}$ and $\|x\|_A = \sqrt{\langle x, x \rangle_A}$ for the induced weighted Euclidean norm. For a measurable space $(\mathbf{E}, \mathcal{E})$, we denote $\mathcal{P}(\mathbf{E})$ as the space of probability measures on $(\mathbf{E}, \mathcal{E})$. For $\mathbb{P}, \mathbb{Q} \in \mathcal{P}(\mathbf{E})$, we define the Kullback–Leibler (KL) divergence from \mathbb{Q} to \mathbb{P} as $\text{KL}(\mathbb{P}|\mathbb{Q}) = \int_{\mathbf{E}} \log(d\mathbb{P}/d\mathbb{Q})d\mathbb{P}$ if \mathbb{P} is absolutely continuous with respect to \mathbb{Q} and the integral is finite, and $\text{KL}(\mathbb{P}|\mathbb{Q}) = \infty$ otherwise. Let $\mathbf{C} = C([0, T], \mathbb{R}^d)$ be the space of continuous functions from $[0, T]$ to \mathbb{R}^d , equipped with the cylinder σ -algebra \mathcal{C} . For each path measure $\mathbb{Q} \in \mathcal{P}(\mathbf{C})$, we

denote the time $t \in [0, T]$ marginal distribution as \mathbb{Q}_t . For $t \in [0, T]$ and $\pi \in \mathcal{P}(\mathbb{R}^d)$, we define the subset $\mathcal{P}_t(\pi) = \{\mathbb{Q} \in \mathcal{P}(\mathbb{C}) : \mathbb{Q}_t = \pi\}$. We will write the path measure induced by (1) with initial condition $X_0 = x_0$ as $\mathbb{P}^{x_0} \in \mathcal{P}_0(\delta_{x_0})$, where δ_x denotes the Dirac measure centered at $x \in \mathbb{R}^d$. In our notation, the marginal distribution $\mathbb{P}_t^{x_0}(dx_t)$ is simply the transition kernel $p(t, dx_t|0, x_0)$. We write $\mathcal{N}(\mu, \Sigma)$ to denote a multivariate normal distribution with mean vector $\mu \in \mathbb{R}^d$ and covariance matrix $\Sigma \in \mathbb{R}^{d \times d}$, and its Lebesgue density as $x \mapsto \mathcal{N}(x; \mu, \Sigma)$.

3 Diffusion bridges

3.1 Time-reversed bridge process

Consider the time-reversed bridge process $Z^* = (Z_t^*)_{t \in [0, T]} = (X_{T-t}^*)_{t \in [0, T]}$. It can be shown that Z^* satisfies the SDE

$$dZ_t^* = b(t, Z_t^*)dt + \sigma(T - t, Z_t^*)dB_t, \quad (5)$$

with initial condition $Z_0^* = x_T$, where the drift function $b : [0, T] \times \mathbb{R}^d \rightarrow \mathbb{R}^d$ is

$$b(t, z_t) = -f(T - t, z_t) + \Sigma(T - t, z_t)s(T - t, z_t) + \nabla \cdot \Sigma(T - t, z_t), \quad (6)$$

$B = (B_t)_{t \in [0, T]}$ is another standard Brownian motion, $s : [0, T] \times \mathbb{R}^d \rightarrow \mathbb{R}^d$ is

$$s(t, x_t) = s^*(t, x_t) - \nabla \log h(t, x_t), \quad (7)$$

and $\nabla \cdot \Sigma(t, x) = (\sum_{j=1}^d \partial_{x_j} \Sigma^{1,j}(t, x), \dots, \sum_{j=1}^d \partial_{x_j} \Sigma^{d,j}(t, x))^\top$ is the divergence of Σ . In the preceding equation, $s^*(t, x_t) = \nabla \log p^*(t, x_t)$ denotes the score of the marginal density $p^*(t, x_t)$ of the diffusion bridge process X_t^* at time $t \in (0, T)$. We refer readers to [Haussmann and Pardoux \(1986\)](#) and [Millet et al. \(1989\)](#) for conditions under which the representation in (5) holds.

By the Markov property, we have the relation

$$p^*(t, x_t) = p(t, x_t | (0, x_0), (T, x_T)) = \frac{p(t, x_t | 0, x_0)h(t, x_t)}{p(T, x_T | 0, x_0)}, \quad (8)$$

as $h(t, x_t) = p(T, x_T | t, x_t)$. This implies that $s(t, x_t) = \nabla_{x_t} \log p(t, x_t | 0, x_0)$ is simply the score of the transition density under the SDE in (1). Approximation of $s(t, x_t)$ will be the focus of Section 3.2. Hence (5) and (6) can be understood as first setting $Z_0^* = x_T$ to satisfy the terminal constraint, and then evolving Z^* using the time-reversal of (1). Due to the influence of the score $s(t, x_t)$, the process will end at the initial constraint $Z_T^* = x_0$ by construction.

It is instructive to consider the time-reversal of (5), which gives

$$dX_t^* = f^*(t, X_t^*)dt + \sigma(t, X_t^*)dW_t, \quad (9)$$

with the initial condition $X_0^* = x_0$ and the drift function $f^* : [0, T] \times \mathbb{R}^d \rightarrow \mathbb{R}^d$

$$f^*(t, x_t) = -b(T - t, x_t) + \Sigma(t, x_t)s^*(t, x_t) + \nabla \cdot \Sigma(T - t, x_t). \quad (10)$$

Using (6) and (7), we can rewrite f^* as

$$f^*(t, x_t) = f(t, x_t) + \Sigma(t, x_t)\{s^*(t, x_t) - s(t, x_t)\} = f(t, x_t) + \Sigma(t, x_t)\nabla \log h(t, x_t), \quad (11)$$

therefore (9) recovers the Doob's h -transformed process in (2). Although this is to be expected as the reversal of the time-reversed process should recover the original process, it forms the basis of our approximation of (2) in Section 3.3.

3.2 Learning time-reversal with score-matching

The observations made in Section 3.1 allow us to cast the task of simulating diffusion bridges as that of time-reversing SDEs. We now introduce a variational formulation to learn an approximation of the time-reversal of (1). Following the form of the time-reversed SDE in (5) and (6), we consider a path measure $\mathbb{Q}_\phi \in \mathcal{P}_0(\delta_{x_0}) \cap \mathcal{P}_T(\mathbb{P}_T^{x_0})$, i.e. with marginal distributions δ_{x_0} and $\mathbb{P}_T^{x_0}$ at time $t = 0$ and T respectively, induced by a time-reversed process $Z = (Z_t)_{t \in [0, T]}$ satisfying

$$dZ_t = b_\phi(t, Z_t)dt + \sigma(T - t, Z_t)dB_t, \quad Z_0 \sim \mathbb{P}_T^{x_0}, \quad (12)$$

with backward drift function $b_\phi : [0, T] \times \mathbb{R}^d \rightarrow \mathbb{R}^d$ defined for $\varepsilon > 0$

$$b_\phi(t, z_t) = -f(T - t, z_t) + \Sigma(T - t, z_t)s_\phi(T - t, z_t) + \nabla \cdot \Sigma(T - t, z_t) + \varepsilon \frac{x_0 - z_t}{T - t}. \quad (13)$$

In the above, $s_\phi : [0, T] \times \mathbb{R}^d \rightarrow \mathbb{R}^d$ denotes an approximation of the score $s(t, x_t)$ that depends on parameters $\phi \in \Phi$ to be inferred. The last term on the right hand side of (13) ensures $\mathbb{Q}_\phi \in \mathcal{P}_0(\delta_{x_0})$, or equivalently $Z_T = x_0$, under appropriate conditions on the behaviour of $s_\phi(t, x_t)$ as $t \rightarrow 0$.

Consider the following KL minimization problem

$$\operatorname{argmin}_{\phi \in \Phi} \operatorname{KL}(\mathbb{P}^{x_0} | \mathbb{Q}_\phi). \quad (14)$$

Assuming that $\operatorname{KL}(\mathbb{P}^{x_0} | \mathbb{Q}_\phi) < \infty$, the Radon–Nikodym derivative of \mathbb{P}^{x_0} with respect \mathbb{Q}_ϕ is given by Girsanov's theorem

$$\frac{d\mathbb{P}^{x_0}}{d\mathbb{Q}_\phi}(Z) = \exp \left\{ -\frac{1}{2} \int_0^T \|b(t, Z_t) - b_\phi(t, Z_t)\|_{\Sigma^{-1}(t, Z_t)}^2 dt + \int_0^T (b - b_\phi)^\top (\Sigma^{-1} \sigma)(t, Z_t) dB_t \right\}. \quad (15)$$

Using properties of Itô integrals and Equations (6) and (13), we can thus write the KL divergence in (14) as

$$\operatorname{KL}(\mathbb{P}^{x_0} | \mathbb{Q}_\phi) = \frac{1}{2} \mathbb{E}^{x_0} \left[\int_0^T \left\| \Sigma(t, X_t) \{s_\phi(t, X_t) - s(t, X_t)\} + \varepsilon \frac{x_0 - X_t}{T - t} \right\|_{\Sigma^{-1}(t, X_t)}^2 dt \right], \quad (16)$$

where \mathbb{E}^{x_0} denotes expectation with respect to \mathbb{P}^{x_0} . The above expression shows how our chosen KL criterion for time-reversing diffusion bridges is related to the notion of score

matching (Hyvärinen and Dayan, 2005; Vincent, 2011). In the context of generative modeling, such connections have been pointed out by Song et al. (2021) and Huang et al. (2021). The form of (16) is not amenable to optimization as it depends on the intractable score $s(t, x_t)$. The following result gives an alternative and practical expression by applying the idea of denoising score matching (Vincent, 2011) to our setting.

Proposition 1. *For any increasing sequence $(t_m)_{m=0}^M$ on the interval $[0, T]$ with $t_0 = 0$ and $t_M = T$, we have $\text{KL}(\mathbb{P}^{x_0} | \mathbb{Q}_\phi) - C_1 + C_2 = \text{L}(\phi)$ for $\text{KL}(\mathbb{P}^{x_0} | \mathbb{Q}_\phi) < \infty$, where the loss function $\text{L} : \Phi \rightarrow \mathbb{R}_+$ is defined as*

$$\text{L}(\phi) = \frac{1}{2} \sum_{m=1}^M \int_{t_{m-1}}^{t_m} \mathbb{E}^{x_0} \left[\left\| s_\phi(t, X_t) - g(t_{m-1}, X_{t_{m-1}}, t, X_t) \right\|_{\Sigma(t, X_t)}^2 \right] dt, \quad (17)$$

the gradient function $g : [0, T] \times \mathbb{R}^d \times [0, T] \times \mathbb{R}^d \rightarrow \mathbb{R}^d$ is

$$g(s, x_s, t, x_t) = \nabla_{x_t} \log p(t, x_t | s, x_s) - \varepsilon \Sigma^{-1}(t, x_t) \frac{x_0 - x_t}{T - t}, \quad (18)$$

for $0 \leq s < t \leq T$ and $x_s, x_t \in \mathbb{R}^d$, and

$$C_1 = \frac{1}{2} \int_0^T \left\| \Sigma(t, x_t) s(t, x_t) - \varepsilon \frac{x_0 - x_t}{T - t} \right\|_{\Sigma^{-1}(t, x_t)}^2 p(t, x_t | 0, x_0) dx_t dt, \quad (19)$$

$$C_2 = \frac{1}{2} \sum_{m=1}^M \int_{t_{m-1}}^{t_m} \mathbb{E}^{x_0} \left[\left\| g(t_{m-1}, X_{t_{m-1}}, t, X_t) \right\|_{\Sigma(t, X_t)}^2 \right] dt, \quad (20)$$

are constants independent of $\phi \in \Phi$.

The proof is given in Appendix A. The important consequence of Proposition 1 is that the variational formulation in (14) is equivalent to minimizing the loss function $\text{L}(\phi)$. This allows us to circumvent the intractable score $s(t, x_t)$ by working with the score of the transition density $p(t, x_t | t_{m-1}, x_{t_{m-1}})$ that appears in (18). Although the latter is also intractable, approximations can be made when the time interval $[t_{m-1}, t_m]$ is sufficiently small. Time-discretizations and other implementation considerations will be discussed in Section 3.4. Lastly, note that the minimal loss is $\text{L}(\phi) = C_2 - C_1$ when we have the exact relation $b_\phi(t, x_t) = b(t, x_t)$. As the constants C_1, C_2 are unknown in practice, the minimal loss will also be unknown.

3.3 Learning Doob's h -transform

Suppose we have found a minimizer $\hat{\phi} \in \arg \min_{\phi \in \Phi} \text{L}(\phi)$ and denote the corresponding score approximation as $\hat{s}(t, x_t) = s_{\hat{\phi}}(t, x_t)$ and backward drift function as $\hat{b}(t, z_t) = b_{\hat{\phi}}(t, z_t)$. Consider a time-reversed bridge process $\hat{Z} = (\hat{Z}_t)_{t \in [0, T]}$ defined by

$$d\hat{Z}_t = \hat{b}(t, \hat{Z}_t) dt + \sigma(T - t, \hat{Z}_t) dB_t, \quad \hat{Z}_0 = x_T, \quad (21)$$

which should be seen as an approximation of (5). Let $\hat{q}(t, z_t | s, z_s)$ denote its transition density for any $0 \leq s < t \leq T$, $\hat{\mathbb{Q}} \in \mathcal{P}_0(\delta_{x_0}) \cap \mathcal{P}_T(\delta_{x_T})$ be the induced path measure and

$\hat{\mathbb{E}}$ to denote expectation with respect to $\hat{\mathbb{Q}}$. Note that $\hat{p}^*(t, x_t) = \hat{q}(T - t, x_t | 0, x_T)$ is an approximation of the marginal density $p^*(t, x_t)$ in (8) for each $t \in (0, T)$.

Our discussion in Section 3.1 prompts having the time-reversal of (21) as an approximation of the Doob's h -transformed process X^* in (2). In particular, under appropriate conditions, the bridge process $\hat{X} = (\hat{X}_t)_{t \in [0, T]} = (\hat{Z}_{T-t})_{t \in [0, T]}$ satisfies

$$d\hat{X}_t = \hat{f}(t, \hat{X}_t)dt + \sigma(t, \hat{X}_t)dW_t, \quad \hat{X}_0 = x_0, \quad (22)$$

with drift function $\hat{f} : [0, T] \times \mathbb{R}^d \rightarrow \mathbb{R}^d$ given by

$$\hat{f}(t, x_t) = -\hat{b}(T - t, x_t) + \Sigma(t, x_t)\hat{s}^*(t, x_t) + \nabla \cdot \Sigma(t, x_t), \quad (23)$$

to be seen as an approximation of f^* in (10). We can approximate the score $\hat{s}^*(t, x_t) = \nabla \log \hat{p}^*(t, x_t)$ of the marginal density $\hat{p}^*(t, x_t)$ and hence the time-reversal of (21) using the methodology described in Section 3.2. Proposition 2 below summarizes the key elements involved, where $\hat{s}_\phi^*(t, x_t)$ denotes our score approximation with parameters $\phi \in \Phi$ to be optimized. Its proof is similar to the proof of Proposition 1 and is thus omitted.

Proposition 2. *Consider a path measure $\hat{\mathbb{Q}}_\phi \in \mathcal{P}_0(\delta_{x_0}) \cap \mathcal{P}_T(\delta_{x_T})$ that is induced by the bridge process $X^\circ = (X_t^\circ)_{t \in [0, T]}$ satisfying*

$$dX_t^\circ = \hat{f}_\phi(t, X_t^\circ)dt + \sigma(t, X_t^\circ)dW_t, \quad X_0^\circ = x_0, \quad (24)$$

with drift function $\hat{f}_\phi : [0, T] \times \mathbb{R}^d \rightarrow \mathbb{R}^d$ given by

$$\hat{f}_\phi(t, x_t) = -\hat{b}(T - t, x_t) + \Sigma(t, x_t)\hat{s}_\phi^*(t, x_t) + \nabla \cdot \Sigma(t, x_t) + \varepsilon \frac{x_T - x_t}{T - t}, \quad (25)$$

for $\varepsilon > 0$ and $\phi \in \Phi$. If $\text{KL}(\hat{\mathbb{Q}}|\hat{\mathbb{Q}}_\phi) < \infty$, for any increasing sequence $(t_m)_{m=0}^M$ on the interval $[0, T]$ with $t_0 = 0$ and $t_M = T$, we have $\text{KL}(\hat{\mathbb{Q}}|\hat{\mathbb{Q}}_\phi) - \hat{C}_1 + \hat{C}_2 = \hat{L}(\phi)$, where the loss function $\hat{L} : \Phi \rightarrow \mathbb{R}_+$ is

$$\hat{L}(\phi) = \frac{1}{2} \sum_{m=1}^M \int_{t_{m-1}}^{t_m} \hat{\mathbb{E}} \left[\left\| \hat{s}_\phi^*(t, \hat{Z}_t) - \hat{g}(t_{m-1}, \hat{Z}_{t_{m-1}}, t, \hat{Z}_t) \right\|_{\Sigma(t, \hat{Z}_t)}^2 \right] dt, \quad (26)$$

and the gradient function $\hat{g} : [0, T] \times \mathbb{R}^d \times [0, T] \times \mathbb{R}^d \rightarrow \mathbb{R}^d$ is

$$\hat{g}(s, z_s, t, z_t) = \nabla_{z_t} \log \hat{q}(t, z_t | s, z_s) - \varepsilon \Sigma^{-1}(t, z_t) \frac{x_T - z_t}{T - t}, \quad (27)$$

for $0 \leq s < t \leq T$ and $z_s, z_t \in \mathbb{R}^d$, and \hat{C}_1 and \hat{C}_2 are constants that do not depend on $\phi \in \Phi$.

As before, Proposition 2 allows us to circumvent intractability in the KL divergence $\text{KL}(\hat{\mathbb{Q}}|\hat{\mathbb{Q}}_\phi)$ by directly minimizing the loss function $\hat{L}(\phi)$. Note that the minimal loss of $\hat{L}(\phi) = \hat{C}_2 - \hat{C}_1$, attained with the exact relation $\hat{f}_\phi(t, x_t) = \hat{f}(t, x_t)$, is also unknown in practice. Other practical implementation issues will be considered in Section 3.4. Given

a minimizer $\phi^\circ \in \arg \min_{\phi \in \Phi} \hat{L}(\phi)$ and the corresponding score approximation $s^\circ(t, x_t) = \hat{s}_{\phi^\circ}^*(t, x_t)$, by rewriting the drift $f^\circ(t, x_t) = \hat{f}_{\phi^\circ}(t, x_t)$ in (25) as

$$f^\circ(t, x_t) = f(t, x_t) + \Sigma(t, x_t) \{s^\circ(t, x_t) - \hat{s}(t, x_t)\} + \varepsilon \left\{ \frac{x_T - x_t}{T - t} - \frac{x_0 - x_t}{t} \right\} \quad (28)$$

and comparing it with (11), we see that the last two terms on the right provide an approximation of the term $\Sigma(t, x_t) \nabla \log h(t, x_t)$ in Doob's h -transform.

3.4 Numerical implementation

We now detail various numerical considerations to implement our proposed methodology. For simplicity, we employ the Euler–Maruyama scheme on a uniform discretization of the interval $[0, T]$, denoted by $0 = t_0 < t_1 < \dots < t_M = T$, with stepsize $\delta t = T/M$ for $M > 1$. Non-uniform discretizations involve only minor modifications; some higher-order schemes could also be considered.

We first consider the procedure in Section 3.1 to learn time-reversals. The time-discretization of the SDE in (1) is given by the following recursion

$$X_{t_m} = X_{t_{m-1}} + \delta t f(t_{m-1}, X_{t_{m-1}}) + \sigma(t_{m-1}, X_{t_{m-1}})(W_{t_m} - W_{t_{m-1}}), \quad (29)$$

for $m \in \{1, \dots, M\}$ with initial condition $X_0 = x_0$. Equation (29) induces a normal approximation of the transition density $p(t_m, x_{t_m} | t_{m-1}, x_{t_{m-1}})$ of the form

$$p_M(t_m, x_{t_m} | t_{m-1}, x_{t_{m-1}}) = \mathcal{N}(x_{t_m}; x_{t_{m-1}} + \delta t f(t_{m-1}, x_{t_{m-1}}), \delta t \Sigma(t_{m-1}, x_{t_{m-1}})). \quad (30)$$

By replacing the score of $p(t_m, x_{t_m} | t_{m-1}, x_{t_{m-1}})$ with that of $p_M(t_m, x_{t_m} | t_{m-1}, x_{t_{m-1}})$, the gradient function $g(t_{m-1}, x_{t_{m-1}}, t_m, x_{t_m})$ in (18) can be approximated by

$$\begin{aligned} g_M(t_{m-1}, x_{t_{m-1}}, t_m, x_{t_m}) & \\ &= -\frac{1}{\delta t} \Sigma^{-1}(t_{m-1}, x_{t_{m-1}}) \{x_{t_m} - x_{t_{m-1}} - \delta t f(t_{m-1}, x_{t_{m-1}})\} - \varepsilon \Sigma^{-1}(t_m, x_{t_m}) \frac{x_0 - x_{t_m}}{T - t_m}. \end{aligned} \quad (31)$$

We then define the following approximation of the loss function $L(\phi)$ in (17)

$$L_M(\phi) = \frac{1}{2} \delta t \sum_{m=1}^M \mathbb{E}_M^{x_0} \left[\left\| s_\phi(t_m, X_{t_m}) - g_M(t_{m-1}, X_{t_{m-1}}, t_m, X_{t_m}) \right\|_{\Sigma(t_m, X_{t_m})}^2 \right], \quad (32)$$

where $\mathbb{E}_M^{x_0}$ denotes expectation with respect to the law of the time-discretized process under (29). To obtain a minimizer $\hat{\phi} \in \arg \min_{\phi \in \Phi} L_M(\phi)$ using stochastic gradient algorithms, the gradient with respect to parameters $\phi \in \Phi$

$$\nabla_\phi L_M(\phi) = \delta t \sum_{m=1}^M \mathbb{E}_M^{x_0} \left[\nabla_\phi s_\phi(t_m, X_{t_m})^\top \Sigma(t_m, X_{t_m}) \{s_\phi(t_m, X_{t_m}) - g_M(t_{m-1}, X_{t_{m-1}}, t_m, X_{t_m})\} \right] \quad (33)$$

can be unbiasedly estimated using independent sample paths from (29). The above notation $\nabla_\phi s_\phi$ refers to the Jacobian of s_ϕ . In Appendix B, we show how $\nabla_\phi \mathbf{L}_M(\phi)$ can be seen as an approximation of the gradient $\nabla_\phi \mathbf{L}(\phi)$.

At this point, we can already simulate proposal bridge paths using the backward drift function $\hat{b}(t, z_t) = b_{\hat{\phi}}(t, z_t)$ defined in (13) and the SDE in (21). Under the Euler–Maruyama scheme, we have

$$\hat{Z}_{t_m} = \hat{Z}_{t_{m-1}} + \delta t \hat{b}(t_{m-1}, \hat{Z}_{t_{m-1}}) + \sigma(T - t_{m-1}, \hat{Z}_{t_{m-1}})(B_{t_m} - B_{t_{m-1}}), \quad (34)$$

for $m \in \{1, \dots, M-1\}$, with initial condition $\hat{Z}_0 = x_T$ and terminal constraint $\hat{Z}_T = x_0$. We will refer to (34) as the time-discretized backward diffusion bridge (BDB) proposal process. Like before, this gives a normal approximation of the transition density $\hat{q}(t_m, z_{t_m} | t_{m-1}, z_{t_{m-1}})$

$$\hat{q}_M(t_m, z_{t_m} | t_{m-1}, z_{t_{m-1}}) = \mathcal{N}(z_{t_m}; z_{t_{m-1}} + \delta t \hat{b}(t_{m-1}, z_{t_{m-1}}), \delta t \Sigma(T - t_{m-1}, z_{t_{m-1}})). \quad (35)$$

We can perform importance sampling (IS) on $\mathbf{E}_M = (\mathbb{R}^d)^{M-1}$ to correct for the discrepancy between the law of BDB

$$\hat{Q}_M(\mathbf{z}_M) = \prod_{m=1}^{M-1} \hat{q}_M(t_m, z_{t_m} | t_{m-1}, z_{t_{m-1}}), \quad \mathbf{z}_M = (z_{t_m})_{m=1}^{M-1} \in \mathbf{E}_M, \quad (36)$$

and the law of the time-discretized diffusion bridge process

$$P_M^*(\mathbf{x}_M) = \frac{\gamma_M(\mathbf{x}_M)}{p_M(T, x_T | 0, x_0)}, \quad \mathbf{x}_M = (x_{t_m})_{m=1}^{M-1} \in \mathbf{E}_M, \quad (37)$$

with $\gamma_M(\mathbf{x}_M) = \prod_{m=1}^M p_M(t_m, x_{t_m} | t_{m-1}, x_{t_{m-1}})$, and also estimate

$$p_M(T, x_T | 0, x_0) = \int_{\mathbf{E}_M} \gamma_M(\mathbf{x}_M) d\mathbf{x}_M, \quad (38)$$

which is an approximation of the transition density $p(T, x_T | 0, x_0)$ under the Euler–Maruyama scheme. The corresponding (unnormalized) importance weight is $\omega(\mathbf{z}_M) = \gamma_M(\mathbf{x}_M) / \hat{Q}_M(\mathbf{z}_M)$ with $\mathbf{x}_M = (z_{T-t_m})_{m=1}^M$, and an unbiased IS estimator of the transition density $p_M(T, x_T | 0, x_0)$ is given by $N^{-1} \sum_{n=1}^N \omega(\mathbf{Z}_M^n)$ where $(\mathbf{Z}_M^n)_{n=1}^N$ denote $N \in \mathbb{N}$ independent sample paths from \hat{Q}_M . As noted by Lin et al. (2010), the root mean squared error of this transition density estimator is approximately equals to the χ^2 -divergence of \hat{Q}_M from P_M^* divided by the sample size N . One can also employ proposals from (36) within an independent Metropolis–Hastings (IMH) algorithm that has (37) as its invariant law (see e.g. Elerian et al. (2001)). At each iteration of the algorithm, a sample path $\mathbf{Z}_M^\circ \sim \hat{Q}_M$ is accepted with probability $\min\{1, \omega(\mathbf{Z}_M^\circ) / \omega(\mathbf{Z}_M)\}$, where \mathbf{Z}_M denotes the current state of the Markov chain. The efficiency of this IMH chain can be assessed by monitoring its acceptance probability. To improve the acceptance probability, we can also combine IMH with IS within a particle independent Metropolis–Hastings (PIMH) algorithm (Andrieu et al., 2010) that has invariant law (37). Each iteration of this PIMH involves selecting a proposed sample path \mathbf{Z}_M° among N candidates $(\mathbf{Z}_M^n)_{n=1}^N \sim \hat{Q}_M$ according to

probabilities proportional to their weights $(\omega(\mathbf{Z}_M^n))_{n=1}^N$, and accepting it with probability $\min\{1, \hat{p}_M^\circ(T, x_T|0, x_0)/\hat{p}_M(T, x_T|0, x_0)\}$ that depends on the ratio of the new and current transition density estimators $\hat{p}_M^\circ(T, x_T|0, x_0) = N^{-1} \sum_{n=1}^N \omega(\mathbf{Z}_M^n)$ and $\hat{p}_M(T, x_T|0, x_0)$, respectively. Under mild assumptions, consistency of IS estimators as $N \rightarrow \infty$ implies that the acceptance probability of PIMH converges to one. PIMH can also be easily combined with unbiased MCMC techniques to provide unbiased estimates of expectations with respect to the law of the time-discretized diffusion bridge (Middleton et al., 2019).

Furthermore, we can learn the Doob’s h -transformed process by following Section 3.3. This is useful in algorithms where one seeks a forward representation of the proposal bridge process (Lin et al., 2010; Del Moral and Murray, 2015; Guarniero, 2017). We sketch the key steps for the sake of brevity. Using the score of the normal transition density in (35), we may approximate the gradient function $\hat{g}(t_{m-1}, z_{t_{m-1}}, t_m, z_{t_m})$ in (27), and hence the loss function $\hat{L}(\phi)$ in (26). The approximate loss can be minimized using stochastic gradient algorithms and sample paths from (34). By time-discretizing the resulting forward diffusion bridge (FDB) proposal process (24), we may then employ it as an importance proposal to approximate the law (37) and the transition density (38), or to generate proposal distributions within IMH and PIMH algorithms.

3.5 Extension to any initial and terminal conditions

Although our exposition has assumed a specific pair of initial and terminal conditions $(x_0, x_T) \in \mathbb{R}^d \times \mathbb{R}^d$, we can extend the proposed methodology to approximate a diffusion bridge process for any arbitrary (x_0, x_T) with some modifications.

Firstly, when learning the time-reversed bridge process in Section 3.2, we let the score approximation $s_\phi(t, x_t)$ of $s(t, x_t)$ also depend on the initial condition x_0 , and average the KL objective in (14) with a distribution $p_0(dx_0)$ supported on \mathbb{R}^d . By applying the arguments of Proposition 1 conditionally on $X_0 = x_0$, we obtain a loss function given by averaging (17) over $p_0(dx_0)$, which can be minimized using time-discretization and stochastic gradient algorithms if sampling from $p_0(dx_0)$ is possible.

After learning the time-reversal, we can also learn Doob’s h -transformed process as in Section 3.3, by extending Proposition 2 to let the score approximation $\hat{s}_\phi^*(t, x_t)$ of $\hat{s}^*(t, x_t)$ now depend on the terminal condition x_T , and averaging the KL objective with a distribution $p_T(dx_T)$ supported on \mathbb{R}^d that can be sampled from. Similar ideas can also be considered to incorporate parameter dependence in f and σ if desired.

4 Numerical examples

In all numerical experiments, we set the constant ε in (13) and (25) as 10^{-3} , and note that our results are not particularly sensitive to ε as long as it is small enough. Although our methodology allows one to employ any function approximator, we will harness the flexibility of neural networks and the ease of implementation using modern software to approximate score functions. The specific network architecture is detailed in Appendix C. All stochastic optimization was performed using ADAM (Kingma and Ba, 2014) for 500 iterations with a momentum of 0.99, learning rate of 0.01 and 100 independent sample paths. Each optimiza-

tion routine took approximately 10 seconds on Intel(R) Core(TM) i7 2.3GHz CPUs, and can be accelerated with the use of GPUs. Note that the cost of learning FDB is approximately twice of BDB as two optimization procedures are required. As such computational overheads are marginal when employing proposal bridge processes within an IS scheme with many samples or IMH and PIMH algorithms with many iterations, we shall focus on assessing the quality of our proposals in settings where existing proposal methods may be unsatisfactory.

We will compare our BDB and FDB methods to the forward diffusion (FD) method of Pedersen (1995), the modified diffusion bridge (MDB) of Durham and Gallant (2002) and the proposal bridge process studied by Clark (1990) and Delyon and Hu (2006) (CDH) on two commonly used examples to test diffusion bridge samplers in the following. We also consider a modification of BDB and FDB, which will be referred to as MBDB and MFDB respectively, that changes the variance of their Euler–Maruyama transitions (see e.g. (35)) with a multiplier of $(T - t_m)/(T - t_{m-1})$ at time step m . This modification can improve practical performance for times near the endpoint by lowering the transition variances. Such behaviour is consistent with findings in earlier works by Durham and Gallant (2002), Papaspiliopoulos and Roberts (2012) and Papaspiliopoulos et al. (2013) when constructing proposals with the drift of a Brownian bridge. Given that it is impossible to compare the wide range of methods for diffusion bridges in a completely fair manner as their strengths and weaknesses depend on the specificities of the problem under consideration, we note that our objective is merely to offer a new perspective to improve the construction of proposal bridge processes.

4.1 Ornstein–Uhlenbeck process

Let X be an Ornstein–Uhlenbeck process, defined by the SDE in (1) with linear drift function $f(t, x_t) = \alpha - \beta x_t$ and identity diffusion coefficient $\sigma(t, x_t) = I_d$. In this analytically tractable example, for any $0 \leq s < t \leq T$, the transition density of X is a normal density $p(t, x_t | s, x_s) = \mathcal{N}(x_t; m(t - s, x_s), v(t - s)I_d)$, with the following mean and variance

$$m(t - s, x_s) = \frac{\alpha}{\beta} + \left(x_s - \frac{\alpha}{\beta}\right) \exp\{-\beta(t - s)\}, \quad v(t - s) = \frac{1 - \exp\{-2\beta(t - s)\}}{2\beta}. \quad (39)$$

Hence the logarithmic gradient term in Doob’s h -transform (2) is

$$\nabla \log h(t, x_t) = \frac{\exp\{-\beta(T - t)\}}{v(T - t)} \{x_T - m(T - t, x_t)\}, \quad (40)$$

and the score of the transition density in (5) is

$$s(t, x_t) = v(t)^{-1} \{m(t, x_0) - x_t\}. \quad (41)$$

We consider dimension $d = 1$, a time interval of $T = 1$, parameters $(\alpha, \beta) = (0, 2)$, the initial and terminal conditions $x_0 = x_T = 1$, and a uniform discretization with $M = 50$ time steps. Figure 1a contrasts the mean and variance of the diffusion transition density and the diffusion bridge marginal density. Notably, sample paths under the diffusion bridge will

initially exhibit mean-reversion towards the origin before being drawn towards the terminal condition at $x_T = 1$. Figure 1b shows how the approximate loss functions evolve during the optimization routines to learn the BDB and FDB processes. As the loss for BDB is smaller than that of FDB, we can expect it to perform better. Figures 1c and 1d allow us to visually inspect the resulting score approximations in this one-dimensional setting. We note that the explosive behaviour of these score functions are reasonably well captured by our choice of neural network.

Table 1 summarizes the numerical performance of all proposal methods considered in terms of their IS effective sample size (ESS), the root mean squared error (RMSE) of their IS transition density estimator, and the acceptance rate of their IMH algorithm. As the FD method proposes sample paths from the original diffusion process (1), its poor performance is evident from Figure 1a. The performance of the popular MDB is highly dependent on the magnitude of β (Stramer and Yan, 2007), which is taken as $\beta = 2$ in this example. The less commonly used CDH performs better than FD but remains unsatisfactory. Our proposed methods perform well in this case, which is unsurprising given Figures 1c and 1d. We also observe substantial improvements using the above-mentioned variance modification, and some accumulation of errors when comparing the forward and backward methods. The latter behaviour is consistent with the difference of loss values in Figure 1b, and to be expected as the forward processes are constructed using an additional score approximation.

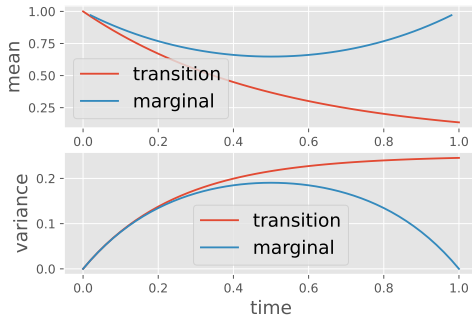
	FD	MDB	CDH	BDB	FDB	MBDB	MFDB
ESS (%)	9.2	52.7	31.6	76.0	72.8	93.9	90.4
RMSE ($\times 10^{-2}$)	9.6	3.2	2.8	1.5	1.9	0.84	1.0
Acceptance (%)	8.6	51.4	46.4	67.8	65.9	86.4	82.4

Table 1: Performance of various proposal methods on the Ornstein–Uhlenbeck example of Section 4.1 based on 1024 IS sample paths or MCMC iterations and 100 independent repetitions of each method.

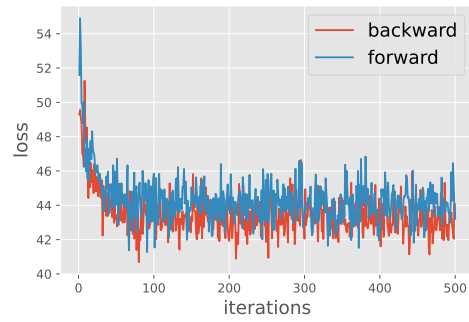
4.2 Periodic drift

Next we consider a diffusion process X defined by the SDE in (1) with a periodic drift function $f(t, x_t) = \alpha \sin(x_t - \theta)$ and $\sigma(t, x_t) = I_d$. As the transition density of X is intractable, so are $\nabla \log h(t, x_t)$ in (2) and $s(t, x_t)$ in (5). Remarkably, the exact algorithm of Beskos and Roberts (2005) and Beskos et al. (2006) can be applied to sample from this diffusion process and its diffusion bridge without any time-discretization error. As our focus is to construct good proposal bridge processes in general settings, accepting discretization errors where necessary, we take the view that a comparison to the exact algorithm would be pointless. We note also that for the task of exact diffusion bridge simulation, the efficiency of such algorithms will depend on the length of the time interval T .

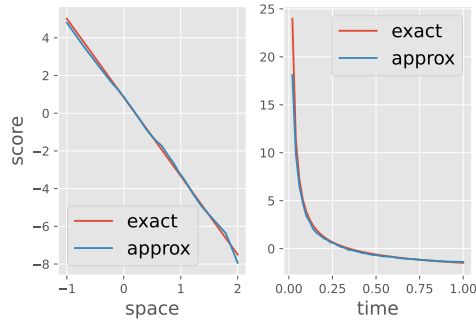
We consider dimension $d = 1$, a time interval of $T = 1$, offset parameter $\theta = \pi$, initial condition $x_0 = 0.1$, terminal condition $x_T = 1$, and a uniform discretization with $M = 50$ time steps. Following previous works, we will set the amplitude parameter as $\alpha = 1$ and also consider $\alpha = 4$ which induces a more challenging setting. In Figure 2a, we see that the behaviour of the approximate loss functions during optimization is similar to Figure 1b for



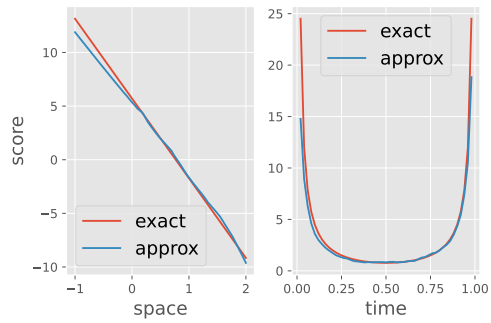
(a) Mean and variance of diffusion transition density (red) and diffusion bridge marginal density (blue).



(b) Approximate loss over ADAM iterations to learn backward (red) and forward (blue) diffusion bridges.



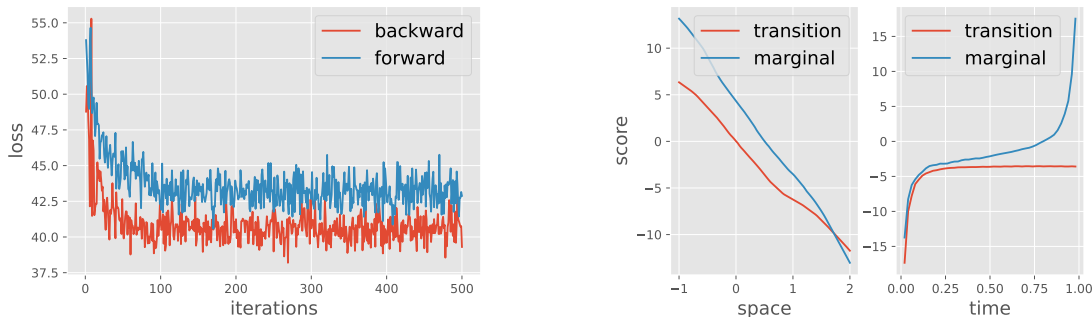
(c) Approximation of score $s(t, x_t)$ at $t = 0.8$ (left) and $x_t = 0.5$ (right).



(d) Approximation of score $s^*(t, x_t)$ at $t = 0.8$ (left) and $x_t = 0.5$ (right).

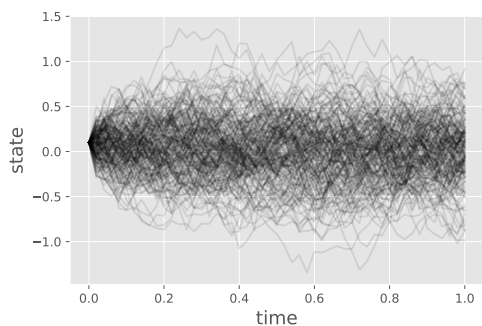
Figure 1: Ornstein–Uhlenbeck example of Section 4.1.

the previous example. The resulting score approximations are plotted in Figure 2b. The time evolution of the diffusion and diffusion bridge processes are contrasted in Figures 2c and 2d.

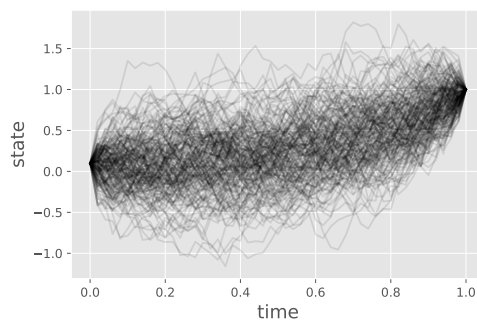


(a) Approximate loss over ADAM iterations to learn backward (red) and forward (blue) diffusion bridges.

(b) Approximation of scores $s(t, x_t)$ (red) and $s^*(t, x_t)$ (blue) at $t = 0.8$ (left) and $x_t = 0.5$ (right).



(c) Sample paths from diffusion process.



(d) Sample paths from BDB.

Figure 2: Periodic drift example of Section 4.2 with amplitude parameter $\alpha = 4$.

Lastly, Table 2 compares all proposal methods using the performance measures introduced above¹. While the conclusions are similar to the previous example, we note that MDB performs well when the amplitude parameter α is smaller. In contrast, the performance of our proposed methods is more robust to the value of α .

¹The RMSE was computed using the IS transition density estimate of MBDB with 262,144 sample paths as reference.

		FD	MDB	CDH	BDB	FDB	MBDB	MFDB
$\alpha = 1$	ESS (%)	10.7	97.4	58.5	73.3	69.9	96.5	92.5
	RMSE ($\times 10^{-2}$)	8.8	0.2	1.4	1.8	2.1	0.6	0.9
	Acceptance (%)	9.9	90.4	58.4	65.9	64.1	90.1	85.4
$\alpha = 4$	ESS (%)	1.9	35.2	21.6	76.5	72.9	86.8	84.7
	RMSE ($\times 10^{-2}$)	24.7	2.1	5.4	1.7	2.0	1.2	1.3
	Acceptance (%)	2.5	38.2	37.2	68.7	65.7	79.6	77.7

Table 2: Performance of various proposal methods on the periodic drift example of Section 4.2 based on 1024 IS sample paths or MCMC iterations and 100 independent repetitions of each method.

5 Discussion

We discuss here some possible refinements and extensions of our proposed methodology. We are currently investigating how our proposed methods behave for higher-dimensional problems. As the drift functions constructed in (12) and (24) are singular near the terminal time, we could employ the time change and scaling techniques proposed by van der Meulen and Schauer (2017) to improve the time-discretization of these processes. Extending this work to facilitate statistical inference in the regime of partial and noisy observations could be considered along the lines of Golightly and Wilkinson (2008). Lastly, we note that our time-reversal methodology can be used to design the backward dynamics required by Takayanagi and Iba (2018) to efficiently estimate the probability of rare events driven by diffusion processes.

Acknowledgements

Valentin De Bortoli and Arnaud Doucet are partly supported by the EPSRC grant CoSInES EP/R034710/1. Jeremy Heng was funded by CY Initiative of Excellence (grant “Investissements d’Avenir” ANR-16-IDEX-0008).

References

- Andrieu, C., A. Doucet, and R. Holenstein (2010). Particle Markov chain Monte Carlo methods (with discussion). *Journal of the Royal Statistical Society: Series B (Statistical Methodology)* 72(3), 269–342. 9
- Arnaudon, A., F. van der Meulen, M. Schauer, and S. Sommer (2020). Diffusion bridges for stochastic Hamiltonian systems with applications to shape analysis. *arXiv preprint arXiv:2002.00885*. 2
- Beskos, A., O. Papaspiliopoulos, and G. O. Roberts (2006). Retrospective exact simulation of diffusion sample paths with applications. *Bernoulli* 12(6), 1077–1098. 3, 12
- Beskos, A., O. Papaspiliopoulos, G. O. Roberts, and P. Fearnhead (2006). Exact and computationally efficient likelihood-based estimation for discretely observed diffusion processes

- (with discussion). *Journal of the Royal Statistical Society: Series B (Statistical Methodology)* 68(3), 333–382. [2](#)
- Beskos, A. and G. O. Roberts (2005). Exact simulation of diffusions. *The Annals of Applied Probability* 15(4), 2422–2444. [3](#), [12](#)
- Beskos, A., G. O. Roberts, A. Stuart, and J. Voss (2008). MCMC methods for diffusion bridges. *Stochastics and Dynamics* 8(03), 319–350. [2](#)
- Bierkens, J., S. Grazi, F. van der Meulen, and M. Schauer (2021). A piecewise deterministic Monte Carlo method for diffusion bridges. *Statistics and Computing* 31(3), 1–21. [2](#)
- Bladt, M., S. Finch, and M. Sørensen (2016). Simulation of multivariate diffusion bridges. *Journal of the Royal Statistical Society: Series B (Statistical Methodology)*, 343–369. [3](#)
- Bladt, M. and M. Sørensen (2014). Simple simulation of diffusion bridges with application to likelihood inference for diffusions. *Bernoulli* 20(2), 645–675. [3](#)
- Bolhuis, P. G., D. Chandler, C. Dellago, and P. L. Geissler (2002). Transition path sampling: Throwing ropes over rough mountain passes, in the dark. *Annual Review of Physical Chemistry* 53(1), 291–318. [2](#)
- Clark, J. M. C. (1990). The simulation of pinned diffusions. In *29th IEEE Conference on Decision and Control*, pp. 1418–1420. IEEE. [2](#), [11](#)
- De Bortoli, V., J. Thornton, J. Heng, and A. Doucet (2021). Diffusion Schrödinger bridge with applications to score-based generative modeling. In *Advances in Neural Information Processing Systems*. PMLR. [3](#)
- Del Moral, P. and L. M. Murray (2015). Sequential Monte Carlo with highly informative observations. *SIAM/ASA Journal on Uncertainty Quantification* 3(1), 969–997. [3](#), [10](#)
- Delyon, B. and Y. Hu (2006). Simulation of conditioned diffusion and application to parameter estimation. *Stochastic Processes and their Applications* 116(11), 1660–1675. [2](#), [11](#)
- Durham, G. B. and A. R. Gallant (2002). Numerical techniques for maximum likelihood estimation of continuous-time diffusion processes. *Journal of Business & Economic Statistics* 20(3), 297–338. [2](#), [11](#)
- Elerian, O., S. Chib, and N. Shephard (2001). Likelihood inference for discretely observed nonlinear diffusions. *Econometrica* 69(4), 959–993. [2](#), [9](#)
- Eraker, B. (2001). MCMC analysis of diffusion models with application to finance. *Journal of Business & Economic Statistics* 19(2), 177–191. [2](#)
- Golightly, A. and D. J. Wilkinson (2008). Bayesian inference for nonlinear multivariate diffusion models observed with error. *Computational Statistics & Data Analysis* 52(3), 1674–1693. [2](#), [15](#)

- Guarniero, P. (2017). *The Iterated Auxiliary Particle Filter and Applications to State Space Models and Diffusion Processes*. Ph. D. thesis, University of Warwick. [3](#), [10](#)
- Hausmann, U. G. and E. Pardoux (1986). Time reversal of diffusions. *The Annals of Probability*, 1188–1205. [4](#)
- Huang, C.-W., J. H. Lim, and A. Courville (2021). A variational perspective on diffusion-based generative models and score matching. In *NeurIPS 2021*. PMLR. [6](#)
- Hyvärinen, A. and P. Dayan (2005). Estimation of non-normalized statistical models by score matching. *Journal of Machine Learning Research* 6(4). [6](#)
- Kingma, D. P. and J. Ba (2014). Adam: A method for stochastic optimization. *arXiv preprint arXiv:1412.6980*. [10](#)
- Lin, M., R. Chen, and P. Mykland (2010). On generating Monte Carlo samples of continuous diffusion bridges. *Journal of the American Statistical Association* 105(490), 820–838. [3](#), [9](#), [10](#)
- Middleton, L., G. Deligiannidis, A. Doucet, and P. E. Jacob (2019). Unbiased smoothing using particle independent Metropolis–Hastings. In *International Conference on Artificial Intelligence and Statistics*. PMLR. [10](#)
- Millet, A., D. Nualart, and M. Sanz (1989). Integration by parts and time reversal for diffusion processes. *The Annals of Probability*, 208–238. [4](#)
- Papaspiliopoulos, O. and G. O. Roberts (2012). Importance sampling techniques for estimation of diffusion models. In M. Kessler, A. Lindner, and M. Sorensen (Eds.), *Statistical Methods for Stochastic Differential Equations*, pp. 311–340. Chapman and Hall/CRC. [2](#), [11](#)
- Papaspiliopoulos, O., G. O. Roberts, and O. Stramer (2013). Data augmentation for diffusions. *Journal of Computational and Graphical Statistics* 22(3), 665–688. [2](#), [11](#)
- Pedersen, A. R. (1995). Consistency and asymptotic normality of an approximate maximum likelihood estimator for discretely observed diffusion processes. *Bernoulli*, 257–279. [2](#), [11](#)
- Pellegrino, T. and P. Sabino (2015). Enhancing least squares Monte Carlo with diffusion bridges: an application to energy facilities. *Quantitative Finance* 15(5), 761–772. [2](#)
- Roberts, G. O. and O. Stramer (2001). On inference for partially observed nonlinear diffusion models using the Metropolis–Hastings algorithm. *Biometrika* 88(3), 603–621. [2](#)
- Rogers, L. C. G. and D. Williams (2000). *Diffusions, Markov processes and Martingales: Volume 2: Itô Calculus*, Volume 2. Cambridge university press. [2](#)
- Schauer, M., F. Van Der Meulen, and H. Van Zanten (2017). Guided proposals for simulating multi-dimensional diffusion bridges. *Bernoulli* 23(4A), 2917–2950. [2](#)

- Song, Y., C. Durkan, I. Murray, and S. Ermon (2021). Maximum likelihood training of score-based diffusion models. In *NeurIPS 2021*. PMLR. 6
- Stramer, O. and J. Yan (2007). On simulated likelihood of discretely observed diffusion processes and comparison to closed-form approximation. *Journal of Computational and Graphical Statistics* 16(3), 672–691. 2, 12
- Stuart, A. M., J. Voss, and P. Wilberg (2004). Conditional path sampling of SDEs and the Langevin MCMC method. *Communications in Mathematical Sciences* 2(4), 685–697. 2
- Takayanagi, S. and Y. Iba (2018). Backward simulation of stochastic process using a time reverse Monte Carlo method. *Journal of the Physical Society of Japan* 87(12), 124003. 15
- van der Meulen, F. and M. Schauer (2017). Bayesian estimation of discretely observed multi-dimensional diffusion processes using guided proposals. *Electronic Journal of Statistics* 11(1), 2358–2396. 2, 15
- Vaswani, A., N. Shazeer, N. Parmar, J. Uszkoreit, L. Jones, A. N. Gomez, Ł. Kaiser, and I. Polosukhin (2017). Attention is all you need. In *Advances in Neural Information Processing Systems*, pp. 5998–6008. 20
- Vincent, P. (2011). A connection between score matching and denoising autoencoders. *Neural Computation* 23(7), 1661–1674. 3, 6
- Wang, S., D. Ramkrishna, and V. Narsimhan (2020). Exact sampling of polymer conformations using Brownian bridges. *The Journal of Chemical Physics* 153(3), 034901. 2, 3
- Whitaker, G. A., A. Golightly, R. J. Boys, and C. Sherlock (2017). Improved bridge constructs for stochastic differential equations. *Statistics and Computing* 27(4), 885–900. 2

A Proof of Proposition 1

By expanding the square in (16), we can decompose the KL divergence as

$$\text{KL}(\mathbb{P}^{x_0} | \mathbb{Q}_\phi) = D_1 + D_2 - D_3 + D_4, \quad (42)$$

where $D_1 = C_1$,

$$D_2 = \frac{1}{2} \sum_{m=1}^M \int_{t_{m-1}}^{t_m} \int_{\mathbb{R}^d} \|s_\phi(t, x_t)\|_{\Sigma(t, x_t)}^2 p(t, x_t | 0, x_0) dx_t dt \quad (43)$$

follows by noting that $\|Ax\|_{A^{-1}}^2 = \|x\|_A^2$, and

$$D_3 = \sum_{m=1}^M \int_{t_{m-1}}^{t_m} \int_{\mathbb{R}^d} \langle s_\phi(t, x_t), s(t, x_t) \rangle_{\Sigma(t, x_t)} p(t, x_t | 0, x_0) dx_t dt, \quad (44)$$

$$D_4 = \sum_{m=1}^M \int_{t_{m-1}}^{t_m} \int_{\mathbb{R}^d} \left\langle s_\phi(t, x_t), \varepsilon \Sigma^{-1}(t, x_t) \frac{x_0 - x_t}{T - t} \right\rangle_{\Sigma(t, x_t)} p(t, x_t | 0, x_0) dx_t dt. \quad (45)$$

We shall examine the term D_3 that depends on the unknown score function $s(t, x_t)$. Firstly, we can write

$$D_3 = \sum_{m=1}^M \int_{t_{m-1}}^{t_m} \int_{\mathbb{R}^d} \langle s_\phi(t, x_t), \nabla p(t, x_t | 0, x_0) \rangle_{\Sigma(t, x_t)} dx_t dt. \quad (46)$$

By differentiating the Chapman–Kolmogorov equation (with respect to the variable x_t)

$$\begin{aligned} \nabla p(t, x_t | 0, x_0) &= \nabla \int_{\mathbb{R}^d} p(t, x_t | t_{m-1}, x_{t_{m-1}}) p(t_{m-1}, x_{t_{m-1}} | 0, x_0) dx_{t_{m-1}} \\ &= \int_{\mathbb{R}^d} \nabla \log p(t, x_t | t_{m-1}, x_{t_{m-1}}) p(t, x_t | t_{m-1}, x_{t_{m-1}}) p(t_{m-1}, x_{t_{m-1}} | 0, x_0) dx_{t_{m-1}}, \end{aligned} \quad (47)$$

we obtain

$$D_3 = \sum_{m=1}^M \int_{t_{m-1}}^{t_m} \mathbb{E}^{x_0} \left[\langle s_\phi(t, X_t), \nabla \log p(t, X_t | t_{m-1}, X_{t_{m-1}}) \rangle_{\Sigma(t, X_t)} \right] dt. \quad (48)$$

By expanding the square in (17) and using Equations (20), (43), (48) and (45), we have

$$L(\phi) = C_2 + D_2 - D_3 + D_4. \quad (49)$$

The claim follows by noting the decomposition in (42).

B Approximating the gradient of loss functions

The gradient of the loss function $L(\phi)$ in (17) with respect to parameters $\phi \in \Phi$ is

$$\nabla_\phi L(\phi) = \sum_{m=1}^M \int_{t_{m-1}}^{t_m} \mathbb{E}^{x_0} \left[\nabla_\phi s_\phi(t, X_t)^\top \Sigma(t, X_t) \{s_\phi(t, X_t) - g(t_{m-1}, X_{t_{m-1}}, t, X_t)\} \right] dt. \quad (50)$$

Under a right Riemann sum approximation of the time integral, we have

$$\nabla_\phi L(\phi) \approx \delta t \sum_{m=1}^M \mathbb{E}^{x_0} \left[\nabla_\phi s_\phi(t_m, X_{t_m})^\top \Sigma(t_m, X_{t_m}) \{s_\phi(t_m, X_{t_m}) - g(t_{m-1}, X_{t_{m-1}}, t_m, X_{t_m})\} \right]. \quad (51)$$

If we then employ the Euler–Maruyama scheme (29) to discretize the SDE in (1) and use the corresponding normal transition (30) to define the approximation $g_M(t_{m-1}, x_{t_{m-1}}, t_m, x_{t_m})$ of $g(t_{m-1}, X_{t_{m-1}}, t_m, X_{t_m})$ as in (31), we obtain the gradient approximation in (33).

C Neural network architecture

Figure 3 illustrates the architecture of a simple neural network for our numerical examples.

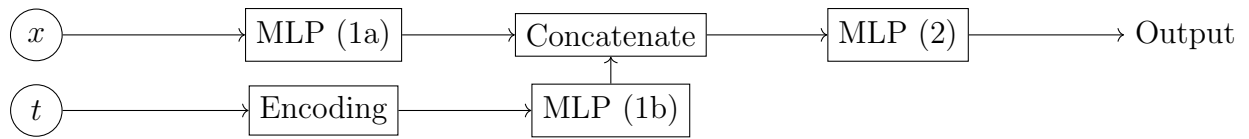


Figure 3: Neural network architecture involves multi-layer perceptron (MLP) blocks and an “Encoding” block which applies the sine transform described in [Vaswani et al. \(2017\)](#). MLP (1a) and (1b) have one hidden layer and MLP (2) has two hidden layers. All neurons use the Leaky ReLU activation function.